Ifeyinwa C. Ekeke[1] , Chukwuebuka E. Mgbemere[2], Charity N. Nwanze[1], Chinedu F. Aniukwu[1], Chigoziri N. Njoku[2]*

[1]Chemical Engineering Department, Federal University of Technology, P. M. B. 1526, Owerri, Imo State, Nigeria.
[2]Environmental, Composite and Optimization Research Group, Department of Chemical Engineering, Federal University of Technology, P. M. B. 1526, Owerri, Imo State, Nigeria.

Scientific paper
ISSN 0351-9465, E-ISSN 2466-2585
https://doi.org/10.62638/ZasMat1266

Zastita Materijala 65 ( )
(2025)

Musa paradisiaca stem sap extract as corrosion inhibitor for aluminum protection in acidic environment

ABSTRACT

This study investigates the efficacy of Musa paradisiaca stem sap extract (MPSSE) as a green corrosion inhibitor for aluminum in a hydrochloric environment. Gas chromatography-mass spectrometry (GC-MS) was used to identify the compounds in the extract. The corrosion inhibition potential was assessed through gravimetric analysis (weight loss measurements) and electrochemical impedance spectroscopy (EIS). Surface analysis was conducted using atomic force microscopy (AFM) to examine the surface morphology of aluminum before and after treatment. Adsorption isotherm studies were performed to understand the interaction mechanism between the extract and the aluminum surface, employing Langmuir, Temkin, Frumkin, and Freundlich isotherms. The results indicate that the extract exhibits significant corrosion inhibition potential. GC-MS analysis identified compounds such as long-chain alkanes, phthalic acid esters, and fluorinated compounds, which contribute to corrosion resistance by forming protective barriers on metal surfaces. Gravimetric analysis showed that the extract, particularly at a 20 V/V% concentration, achieved up to 90.73% inhibition efficiency over 30 days, significantly reducing weight loss and corrosion rates. Adsorption studies revealed a strong adherence to the Temkin Isotherm model, suggesting effective adsorption of the extract onto the aluminum surface. AFM analysis demonstrated a decrease in surface roughness with increasing extract concentration, confirming the inhibitor's protective effect. Electrochemical impedance spectroscopy exhibited higher charge transfer resistance and pronounced inductive behavior in the presence of the inhibitor, indicating the formation of a protective layer on aluminum. These findings highlight the potential of MPSSE as an eco-friendly alternative for corrosion protection in industrial applications.
Keywords: *Corrosion inhibitor: gravimetric analysis; Musa paradisiaca; electrochemical impedance spectroscopy, eco-friendly alternative.*

1. INTRODUCTION

Aluminum is a very useful metal that is known for having a special blend of beneficial qualities. Its remarkable flexibility and lightweight design are two of these that stick out. Aluminum has remarkable reflectivity, excellent ductility, and electrical and thermal conductivity [1. 2]. Because of these qualities, it is an essential material for many applications, such as the production of shell and tube heat exchangers [3]. Aluminum's excellent thermal conductivity makes it ideal for producing heat exchangers with exceptional efficiency since it facilitates efficient heat transfer between various mediums [4]. Shell and tube heat exchangers are essential in the food, chemical, and oil and gas industries [5 - 7]. Heat recovery from exhaust gases and its transfer to liquids is the purpose of this device. This procedure is crucial for condensate recovery, waste heat recovery, and energy recovery [8 – 10]. It also greatly reduces energy consumption and expenses associated with industrial processes. Aluminum performs well in these applications because it can withstand a wide range of temperatures without losing structural integrity.

These heat exchangers are essential in the chemical industry for controlling reaction temperatures, product separation, and energy recovery from process streams [11, 12]. They are employed in the food business to regulate temperature, sterilize, and pasteurize a variety of

*Corresponding author: Ifeyinwa C. Ekeke
E-mail: ifeyinwaekeke@gmail.com
Paper received: 13. 10. 2024.
Paper accepted: 21. 11. 2024.
the website: https://www.zastita-materijala.org/

items. Heat exchangers are essential to the oil and gas sector for the manufacturing of petrochemicals, gas processing, and refining [13]. Heat exchangers in these various industries encounter many difficulties despite the advantages, one of them being corrosion which has become one ubiquitous problem that jeopardizes the equipment's integrity and performance [14]. This equipment works in harsh conditions with high temperatures, corrosive fluids, and chemical interactions, all of which can hasten the corrosion process [15]. Corrosion raises maintenance costs and downtime by causing material degradation, decreased thermal efficiency, and possible system breakdowns [16].

The main causes of corrosion in heat exchangers are specific chemical agents and exposure to corrosive conditions [17]. Corrosive reactions can occur when aluminum interacts with other compounds, particularly acids. For example, hydrochloric and sulfuric acids are frequently used in industrial processes and can seriously corrode aluminum surfaces when they come into touch with them [18]. Secondly, the pace of chemical reactions, especially those that lead to corrosion, is accelerated by high temperatures. High operating temperatures in heat exchangers can accelerate material degradation by aggravating the corrosion process [19]. Also, these heat exchangers can be severely impacted by fluids with high degrees of acidity, salinity, or other corrosive qualities [20] For instance, saltwater used for cooling in some industrial processes has high concentrations of salts that can cause corrosion. Lastly, industrial cleaning processes, such as pickling and acid cleaning, involve the use of hydrochloric acid (HCl) to remove oxides, scale, and rust from metal surfaces [21]. While these processes are essential for maintaining efficiency, they also expose aluminum to aggressive acidic environments, which can initiate and propagate corrosion over time.

Numerous mitigating measures have been devised and put into practice to counteract corrosion in heat exchangers. These tactics seek to preserve effective operation, increase the equipment's longevity, and safeguard the metal surfaces. Typical ways for mitigating include applying protective coatings to aluminum surfaces [22, 23],cathodic protection techniques using sacrificial anodes made of a more reactive metal to protect aluminum surfaces prevent corrosion [24], choosing corrosion-resistant materials for heat exchanger construction to reduce the risk of corrosion [25], and corrosion inhibitors which are added to the fluid streams to reduce the rate of corrosion [26, 27].

The application of corrosion inhibitors is unique among corrosion prevention techniques for a number of reasons. Chemical substances known as corrosion inhibitors are added to a fluid and dramatically lower the pace at which metals exposed to the fluid corrode [28]. Inhibitors are known to be cheap, highly efficient as they provide continuous protection by forming a dynamic protective layer that adapts to changes in the operating environment, and better ease of application as they can be added directly to the process fluids, making them easy to apply and integrate into industrial processes [39, 30]. In recent years, there has been a growing interest in using plant extracts as corrosion inhibitors [31]. Plant extracts offer a sustainable and eco-friendly alternative to conventional chemical inhibitors. They are derived from natural sources and contain a variety of compounds, including phytochemicals, that contribute to their inhibitory properties [32 - 34]. Plant extracts contain key phytochemical compounds that make them effective corrosion inhibitors for instance: alkaloids, which are nitrogen-containing compounds that can adsorb onto metal surfaces and form a protective barrier that prevents corrosion [35]; flavonoids, which are known for their antioxidant properties and can neutralize reactive species that contribute to corrosion [36]; tannins, which are polyphenolic compounds that can form complexes with metal ions, reducing their reactivity and preventing corrosion [37, 38]; and saponins, which are surface-active agents that can form a protective film on metal surfaces, all of which can inhibit corrosion [39].

Musa Paradisiaca, commonly known as plantain, is a type of banana plant that is widely cultivated in tropical regions, including Nigeria. It is a significant crop in Nigerian agriculture, valued for its nutritional and economic contributions [40, 41]. The plantain plant is characterized by its large, green leaves and clusters of fruit, which are typically cooked before consumption. In Nigeria, plantains are a staple food and are grown in various regions, including the southeastern and southwestern parts of the country [42]. *Musa paradisiaca*'s natural phytochemicals are used in an inventive way when used as a corrosion inhibitor. Research has indicated that a range of chemicals with possible anti-corrosion effects can be found in plantain plant extracts [43, 44]. These substances can adsorb onto metal surfaces, creating a layer of defense that lessens the metal's reactivity and prevents corrosion. *Musa paradisiaca* has several benefits when used as a corrosion inhibitor, including affordability, ease of use, and environmental friendliness. Because they are widely cultivated, plantains are readily available, making their extracts an affordable option for industrial applications. Furthermore, the use of

inhibitors derived from plants is consistent with the increasing focus on sustainability and the mitigation of chemical pollutants in industrial processes.

Herein, a combined analytical and electrochemical approach is adopted to evaluate the inhibition properties of *Musa paradisiaca* stem sap extract (MPSSE). The compounds contained in the MPSSP were identified using Gas Chromatography-Mass Spectrometry (GC-MS) analysis. The inhibition efficiencies and corrosion rates were assessed through gravimetric analysis (weight loss) and Electrochemical Impedance Spectroscopy (EIS) techniques. The best adsorption isotherm for the inhibition process was determined by studying the interaction between the MPSSE molecules and the aluminum surface. Additionally, surface analysis of the aluminum coupons before and after inhibition was conducted using Atomic Force Microscopy (AFM) to evaluate the extent of surface roughness and corrosion inhibition. Thermodynamic calculations were employed to understand the inhibitory mechanism, and Langmuir, Temkin, Frumkin, and Freundlich isotherms were used to further study the adsorption behavior of the MPSSE molecules on the metal surface. This study aims to provide a current understanding of the principles driving corrosion inhibition and offer new methods for developing more efficient and environmentally friendly metal corrosion prevention systems.

2.0. EXPERIMENTAL

2.1. Preparation of the Aluminum Samples

The aluminum (Al) plate obtained from Owerri, Imo State, Nigeria was used as test material. Sample coupons of 1 cm x 1cm x 1cm were cut to assemble the working electrodes to be used in the electrochemical studies, while sample coupons of varied dimensions such as D_2(6 cm × 1.2 cm × 0.05 cm); D_4(5.9 cm x 1.1 cm x 0.1 cm); D_7(6 cm × 1 cm ×0.05 cm);); D_9(5.8 cm × 1.1 cm × 0.1 cm); D_{11}(6.2 cm × 1.1 cm × 0.05 cm); D_{12}(6 cm × 1.1 cm × 0.07 cm) were used for weight loss tests. The aluminum coupons were cleaned by dry polishing using emery paper before being degreased with acetone, then dried at room temperature before use.

2.2 .Preparation of the Extract

The MPSSE was prepared in two ways which are, the mechanical/manual extraction, and the solvent extraction method (using a Soxhlet extractor). The *Musa paradisiaca* stems were obtained commercially in Owerri, Imo State. The stems were cut into smaller pieces, ground and mashed with lab. mortar, then placed in a sanitized bag filter with micro-size pores. The liquid extract was afterwards pressed into a clean basin at room temperature.

The second method made use of a Soxhlet extractor. The extractor included an extraction chamber, condenser, thimble, siphon arm, and glass body with a round bottom distillation flask. The plantain stems were washed with distilled water, sliced into smaller pieces, and exposed to the sun for seven days. 12.9 g of the stems were extracted in a Soxhlet apparatus with 250 ml of n-hexane at 78°C till exhaustion solvent was recovered; extracts were concentrated and allowed to dry at room temperature [45].

2.3. Preparation of the Inhibitor Concentrations

Different concentrations of the MPSSE were prepared from the stock solution. Five inhibitor concentrations (25ml, 50ml, 75ml, 100ml, and 125ml of the extract in HCl solution) were prepared using volume per volume method to give 5.88 V/V%, 11.11 V/V%, 15.79 V/V%, 20 V/V%, and 23.81 V/V% of extract concentration.

2.4. Gas Chromatography-Mass Spectroscopy

The chemical composition of the Musa Paradisiaca extract was characterized using Gas Chromatography-Mass Spectrometry (GC-MS). The analysis was performed with an Agilent 5977B GC/MSD system coupled with an Agilent 8860 auto-sampler. The GC-MS system was equipped with an Elite-5MS fused capillary column. For the GC-MS detection, an electron ionization system was operated in electron impact mode with an ionization energy of 70 eV. High-purity helium gas (99.999%) was used as the carrier gas at a constant flow rate of 1 ml/min. An injection volume of 1 µl was used, with a split ratio of 10:1. The injector temperature was set at 300 °C, while the ion-source temperature was maintained at 250 °C.

The oven temperature program was as follows: starting at 100 °C (isothermal for 0.5 min), increasing at a rate of 20 °C/min to 280 °C, and holding at this final temperature for 2.5 min. Mass spectra were acquired at 70 eV, with a scanning interval of 0.5 s, and mass fragments were detected in the range of 45 to 450 Da. The solvent delay was set from 0 to 3 min to avoid interference from the solvent peak.

2.5. Gravimetric Analysis

The gravimetric tests were performed at different inhibitor concentrations, and time intervals. The weight loss measurements were conducted by placing the Al coupons in separate cylindrical plastic containers with 400 ml of 0.5 M HCl solution. Then the Al coupons were also individually submerged in cylindrical containers with 400 ml of the different concentrations of

MPSSE (5.88 V/V%, 11.11 V/V%, 15.79 V/V%, 20 V/V%, and 23.81 V/V%).

First, the coupons were suspended in the container after being weighed with an electronic balance. Over the course of thirty (30) days, the coupons were recovered every three days, carefully cleaned with a brush, rinsed several times in water, dried and then reweighed. The weight losses were obtained by the differences between the initial and final weights. The weight loss (ΔW), corrosion rate (CR), inhibition efficiency (%IE) and surface coverage (θ) were calculated by using the following Eqs. (1-4):

$$\triangle W = W_i - W_f \quad (1)$$

$$CR = \frac{\triangle W}{A \times t} \quad (2)$$

$$\% IE = \frac{CR_O - CR_i}{CR_O} \times 100 \quad (3)$$

$$\theta = \frac{IE}{100} \quad (4)$$

where; $\triangle W$ is the weight loss of coupon (g), W_i is the initial weight loss (g), W_f is the weight of coupon at any time of observation (g), CR is the corrosion rate (g/cm^{2}day), A is the area of coupon (cm^2), t is the time of immersion (day), % IE is the inhibition efficiency, CR_O is the corrosion rate of coupon before inhibition (g/cm^{2}day), CR_i is the corrosion rate of coupon after inhibition (g/cm^{2}day), θ is the surface coverage.

2.6. Adsorption Isotherms

The method by which inhibitors adsorb on the metal surface is described by adsorption isotherm investigations [46]. By fitting the concentration (V/V%) and surface coverage (θ) of the inhibitor into the various adsorption isotherm models (Langmuir, Temkin, Frumkin, and Freundlich adsorption isotherms), the adsorption isotherm model that best described the adsorption of MPSSE on aluminum in 0.5M HCl medium was determined. The relationship between surface coverage (θ) and concentration (V/V%) is provided by the following equations of the various isotherms' Eqs. (5 -8):

Langmuir isotherm:

$$\frac{C_{inh}}{\theta} = C_{inh} + \frac{1}{K_{ads}} \quad (5)$$

Temkin isotherm:

$$\theta = \frac{2.303}{\alpha}\left(\log K_{ads} + \log C_{inh}\right) \quad (6)$$

Frumkin isotherm:

$$\frac{\theta}{1-\theta} = K_{ads} C_{inh} e^{2a\theta} \quad (7)$$

Freundlich isotherm:

$$\log \theta = n \log C_{inh} + \log K_{ads} \quad (8)$$

where C_{inh} is the concentration of the inhibitor, K_{ads} is the adsorption constant, α and a are constants. n is a slope.

2.7. Electrochemical Impedance Spectroscopy (EIS) Analysis

A three-electrode cell with an aluminum working electrode, a platinum auxiliary electrode, and a saturated calomel electrode (SCE) as the reference electrode was used for the electrochemical studies. In this study, all potential values are stated in relation to the SCE. The trials were conducted both with and without the MPSSE. EIS measurements were carried out in the frequency range of 100 kHz to 20 MHz, by applying 5mV amplitude.

2.8. Atomic Force Microscopy (AFM) Analysis

6 of the aluminum coupons used for the weight loss analysis; the first from the blank HCl solution, and each of the rest from the five inhibitor solutions (I,e, the solutions containing 5.8 V/V%, 11.11 V/V%, 15.89 V/V%, 20 V/V%, 23.81 V/V%) were employed for the AFM analysis. An atomic force microscope (Stromlingo DIY AFM model) was used to observe the metal surfaces.

3. RESULTS AND DISCUSSION

3.1.Gas Chromatography Mass Spectroscopy Analysis

The extract from the *Musa paradisiaca* stem sap showed twenty-four (24) identified compounds as seen in Table 1.

Table 1: *Volatile Phytochemical Composition (GC-MS) of Musa Paradisiaca Stem Sap*

S/N	RT	Area%	Compound Name	% Composition
1	7.058	2.99	Phthalic acid, pentadecyl 2-propylphenyl ester	2.99
2	8.918	3.91	Eicosane	3.91
3	11.121	7.66	2-methyltetracosane	7.66
4	11.499	5.19	Octacosane	5.19
5	12.18	3.17	Tetrapentacontane	3.17
6	12.912	5.42	Octadecane	5.42
7	14.148	3.42	Octatriacontyl pentafluoropropionate	3.42
8	14.245	3.71	Tetrapentacontane	3.71
9	14.388	2.87	Hexacosane	2.87
10	14.526	4.2	Octatriacontyl pentafluoropropionate	4.20
11	14.571	4.87	Nonacosane	4.87
12	14.846	2.78	Hentriacontane	2.78
13	15.167	4.93	Hentriacontane	4.93
14	15.51	4.36	Heptacosane	4.36
15	15.55	3.8	Octacosane	3.80
16	15.756	5.41	Tricosane	5.41
17	16.179	3.9	Octacosane	3.90
18	16.74	2.81	Octacosane	2.81
19	16.912	3.39	Hexatriaconyl pentafluoropropionate	3.39
20	17.083	5.32	Tetracosane	5.32
21	17.101	5.42	Hentriacontane	5.42
22	17.57	3.12	Octatriacontyl trifluoroacetate cyclotetradecane	3.12
23	18.857	4.27	Octacosane	4.27
24	19.864	3.09	Hexacosane	3.08

The GC-MS analysis of the MPSSE revealed a diverse array of compounds with significant potential for corrosion inhibition. Each peak and its corresponding retention time represent a specific component of the sample quantified in their percentage composition. Long chain alkanes (such as Eicosane, Octacosane, Hentriacosane, and Tricosane with abundant composition in the sap extract) are commonly found in plant waxes and cuticles [47]. They can form protective layers on metal surfaces, shielding them from corrosive agents. These compounds also contribute to the overall effectiveness of the sap in inhibiting corrosion. Phthalic acid, pentadecyl-2-propylphenyl ester present in the extract, can adsorb onto the metal surface and form a protective barrier. The long hydrophobic alkyl chain (pentadecyl) allows the molecule to adsorb onto the metal surface, creating a barrier that shields the metal from corrosive agents. Additionally, the aromatic phenyl group and the phthalic acid moiety may interact with the metal surface, further enhancing the

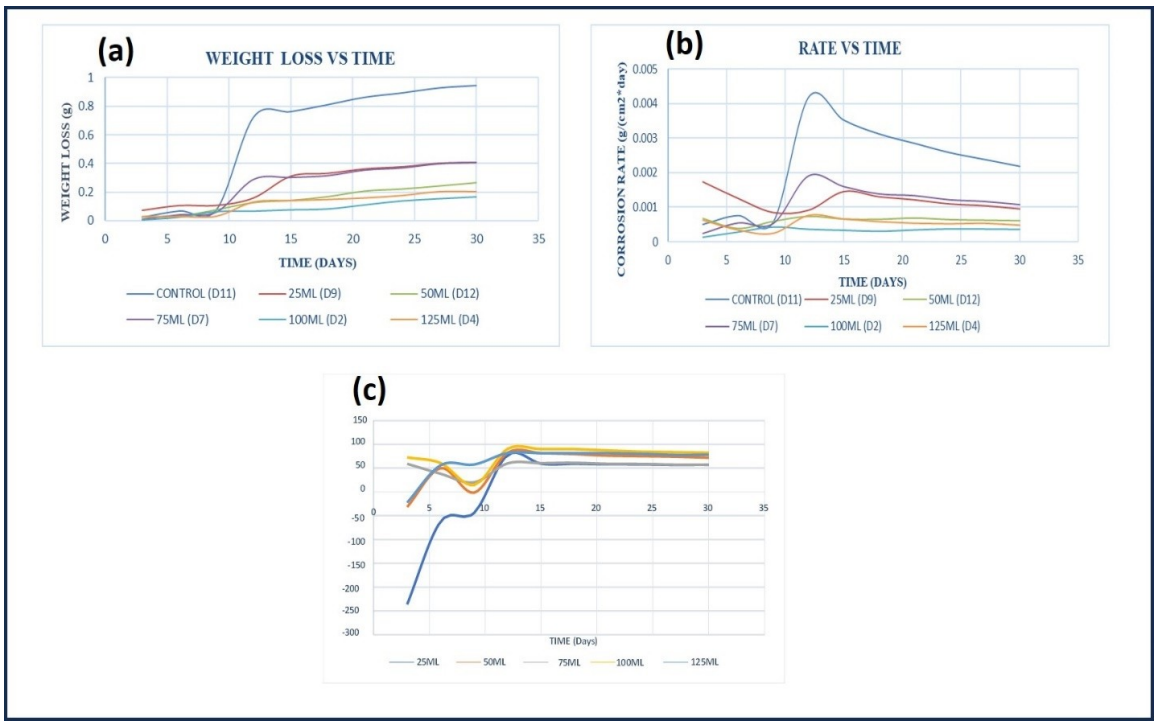

Figure 1: *Plots of aluminum coupons in 0.5M HCL solution for;* ***(a)*** *weight loss (g) vs. time (day);* ***(b)*** *Corrosion rate vs. time and* ***(c)*** *Inhibition Efficiency (%) vs time*

protective effect. Moreover, Hexatriacontyl pentafluoropropionate,Octatriacontyl rifluoroacetate cyclotetradecane and Octatriacontyl pentafluoropropionate present in the sap extract are long-chain fluorinated compounds used as a corrosion inhibitor. Their effectiveness in inhibiting corrosion is primarily attributed to the presence of fluorine atoms in the molecule. Fluorine is highly electronegative, which means it can form strong bonds with other atoms, making the compound less susceptible to oxidation and corrosion. Additionally, the long carbon chain in these compounds provides a hydrophobic barrier, preventing water and other corrosive substances from reaching the surface of the metal, further inhibiting corrosion.

In summary, the inhibitive nature of MPSSE can be attributed to the presence of Phthalic acid esters, fluorinated compounds, long-chain alkanes, and other organic compounds. These compounds, which possess relatively high molecular weights and consist of long chains of carbon atoms bonded together, have non-polar characteristics that enable them to form protective films on metal surfaces.

3.2. Gravimetric Analysis

Results of weight loss measurements in the acid media without and with the addition of various concentrations of MPSSE are shown in Fig. 1a.

The graph of weight losses clearly reveals that the control sample experienced the highest weight losses over the experimental period, though it shows lower values before the 8th day. This is also evident in the corrosion rate versus time graph. The sample containing 100ml of the inhibitor had the lowest weight loss and corrosion rates over the period of observation. This invariably means that this sample also had the highest inhibition efficiency values as can be seen in Fig. 1c, though it occurred from somewhere about the 12th day. The 125ml sample experienced the next lower weight loss values and hence the next values of inhibition efficiency after the 100ml sample. This trend also became obvious from the 12th day of the experimentation. The inhibition efficiency graphs show that, generally, inhibition efficiency values above 50% were obtained for this extract from the 12th day to the end of the experiments for all the concentrations. These results prove the extract's ability to significantly reduce the corrosion rate of the aluminum metal in HCl medium.

3.3. Adsorption Isotherm Parameters

The adsorption mechanism of the inhibitors was examined through the application of Langmuir, Temkin, Frumkin, and Freundlich isotherms. The graph of C/θ_{avg} vs C for Langmuir adsorption is displayed by the isotherm, as shown in Fig. 2a. The correlation coefficient (R^2) was utilised to find the

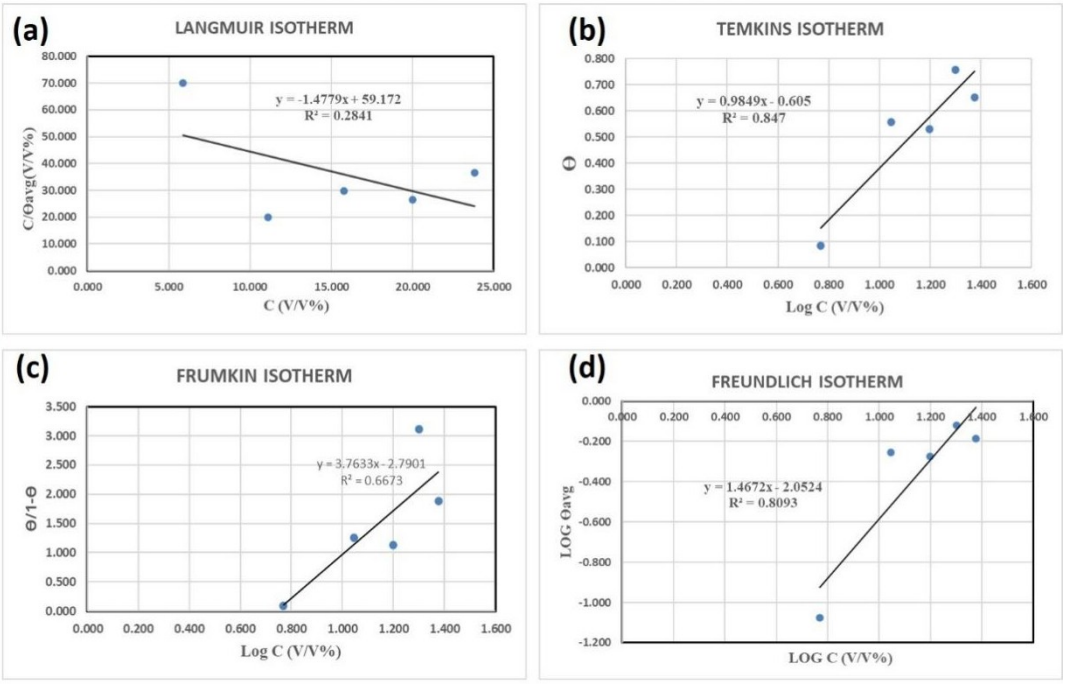

Figure 2: *Different isotherm plots of MPSSE for the corrosion of Al in HCl for;* ***(a)*** *Langmuir,* ***(b)*** *Temkin* ***(c)*** *Frumkin, and* ***(d)*** *Freundlich*

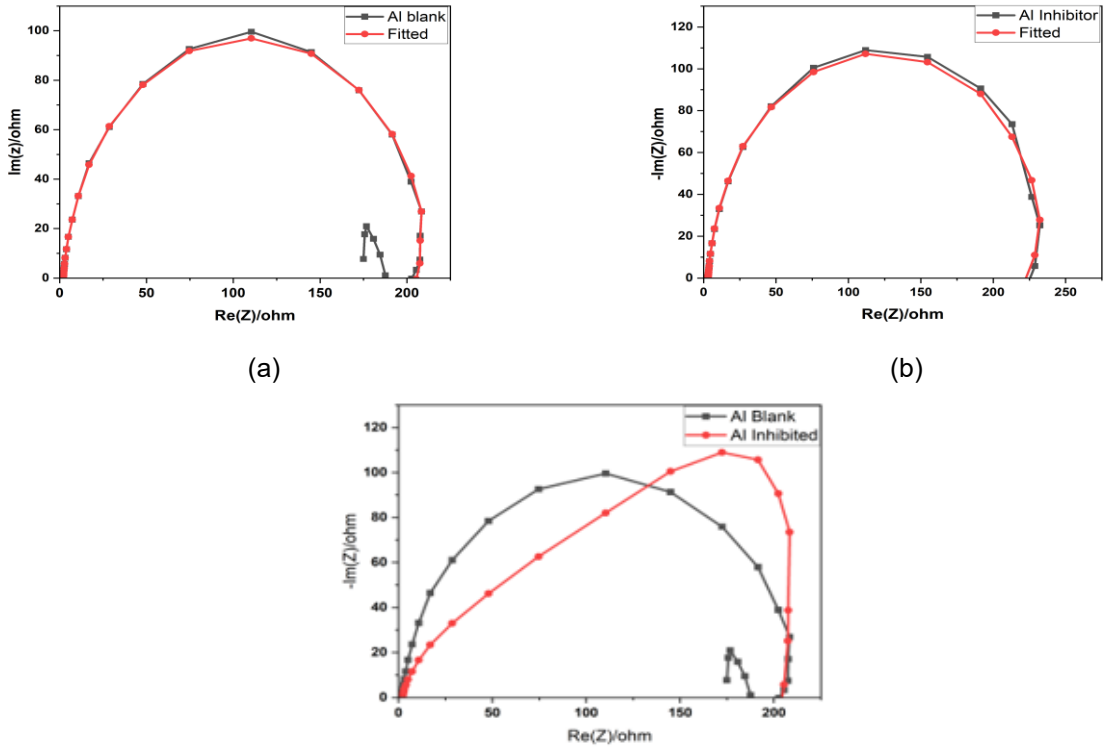

Figure 3: *Nyquist representations of experimental data and results of electrode impedance for Al/0.5 M HCl in the absence and the presence of the inhibitor.*

best fit and ascertain the mode of adsorption of the *Musa paradisiaca* stem sap extract onto the aluminum surface. The surface coverage data were easily fitted into the selected adsorption isotherms. With a low regression coefficient of 0.2841, the graph could not fit the Langmuir adsorption isotherm, indicating limited adherence to the isotherm. Fig. 2b displays the Temkin isotherm graph. The graph reveals a strong adherence to the isotherm as evidenced by a best fit with the linear plot regression coefficient (R^2) with a value of 0.847. Fig. 2c shows the graph of Frumkin isotherm. The graph shows a slightly much better adherence to the isotherm than the Langmuir adsorption Isotherm resulting from a best fit with the linear plot regression coefficient (R^2) with a value of 0.6673. Fig. 2d represents the graph of the Freundlich Isotherm, showing log average vs. Log C. An R^2 value of 0.8093 was obtained suggesting a good fit. A comparison of the various isotherms shows that the Temkin adsorption isotherm gave the best linear relationship which indicates that the inhibitor was strongly adsorbed on the metal surface following the Temkin model as its R^2 value was closest to unity (1).

3.4. Electrochemical Impedance Spectroscopy Analysis

EIS measurements were performed to examine the corrosion inhibition process at the metal/solution interface, which allows us to gain deeper insight into the inhibition processes. Figs. 3 and 4 display impedance spectra collected at room temperature and MPSSE concentration.

In the high-frequency region, both curves start near the origin, indicating that the solution Resistance (R_s) is low and similar for both cases (Fig. (3a)). In the mid-frequency region, the black curve (Al Blank) shows a semicircle that peaks around 80 ohms on the imaginary axis. In contrast, the red curve (Al Inhibited) exhibits a semicircle that peaks around 100 ohms on the imaginary axis, suggesting a different electrochemical behavior when the inhibitor is present (refer to Fig. (3b)). In the low-frequency region, after the main semicircle, the black curve (Al Blank) dips downward and shows small fluctuations. This behavior is indicative of inductive effects, often associated with the adsorption of intermediates or relaxation processes on the electrode surface (refer to Fig. 3c). Similarly, the red curve (Al inhibited) dips down after the main semicircle, showing a more pronounced dip compared to the blank, which is also indicative of inductive behavior. The charge transfer resistance (R_{ct}) can be analyzed based on the semicircle sizes in the EIS spectra. For the Al Blank sample, the smaller semicircle indicates a lower charge transfer resistance, suggesting a more active corrosion process in the absence of the inhibitor. Conversely, for the Al inhibited sample, the larger semicircle indicates a higher charge transfer resistance. This suggests that the inhibitor effectively increases the resistance to charge transfer, likely by forming a protective layer on the aluminum surface, which slows down the corrosion process. The double layer capacitance (Q1) can be inferred from the size of the semicircles in the EIS spectra. For the Al Blank sample, the smaller semicircle may indicate a lower double-layer capacitance. In contrast, the Al Inhibited sample shows a larger semicircle, which may suggest a higher double-layer capacitance due to the formation of a more stable and possibly thicker protective layer. The inductive behavior observed at low frequencies is characterized by a downward dip in both the Al Blank and Al Inhibited curves, forming what is referred to as an inductive loop. This behavior is typically caused by the adsorption of species onto the electrode surface or relaxation processes in the system. For the Al Blank sample, the presence of a small inductive loop suggests some degree of adsorption or relaxation processes taking place without the inhibitor. In comparison, the Al inhibited sample exhibits a larger inductive loop, indicating more significant adsorption or relaxation effects when the inhibitor is present. This could be due to the inhibitor causing the formation of intermediate species that adsorb onto the electrode surface.

From Fig. 4a, at low frequencies (around 0.1 Hz to 1 Hz), the magnitude remains relatively high and stable, indicating that the impedance is relatively high. As the frequency increases (from around 10 Hz to 1 kHz), the magnitude decreases significantly, showing a drop in impedance. Beyond 1 kHz, the magnitude levels off, indicating that the impedance becomes less frequency-dependent at higher frequencies. At low frequencies (around 0.1 Hz to 1 Hz), the phase angle is around 0^o, indicating that the voltage and current are in phase. As the frequency increases (from around 1 Hz to 10 Hz), the phase angle decreases, reaching around -10^o, indicating a slight lag of current behind voltage. From 10 Hz to 1 kHz, the phase angle drops more steeply, reaching around -80^o, indicating a significant lag of current behind voltage. From Fig. 4b, at low frequencies (around 0.1 Hz to 1Hz), the magnitude is relatively high and stable, indicating that the impedance is relatively high. As frequency increases, the magnitude decreases significantly, showing a drop in impedance. And, at low frequencies (0.1 Hz to 1 Hz), the phase angle starts around -20^o, indicating some lag of current behind voltage. As the frequency increases, the phase angle decreases, reaching around -70^o.

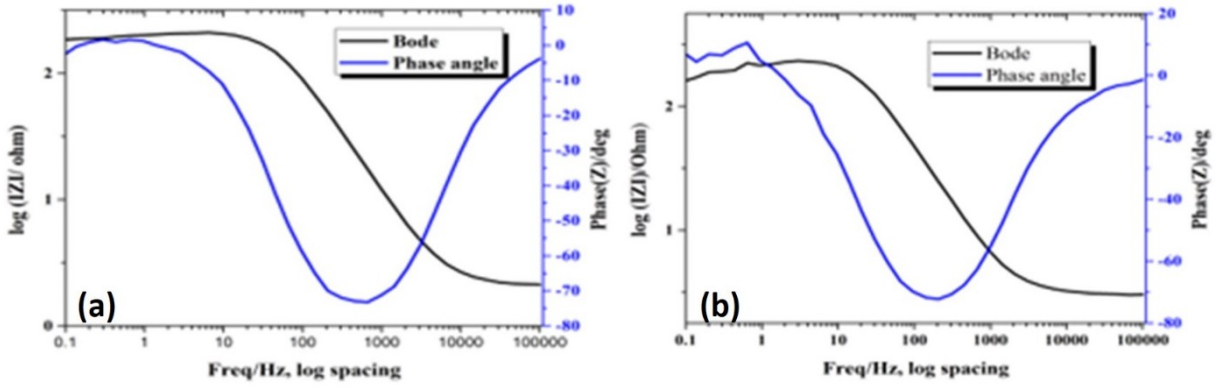

***Figure 4**: Graphical representation showing the Bode plot and Phase angle of Aluminum Coupon immersed in (a) blank solution and (b) solution containing inhibitor.*

***Table 2:** AFM data for aluminum surface immersed in uninhibited and inhibited environment.*

Samples	**RMS Roughness**	**Average Roughness**	**Maximum height (Sz)**
1. Aluminum coupon (D_{11}) immersed in HCl acid solution (blank)	183.917 pm	0.56355 nm	1.34769 nm
2. Aluminum coupon (D_9) immersed in HCl acid solution containing 5.88 V/V% of extract	53.8324 pm	0.56355 nm	1.20639 nm
3. Aluminum coupon (D_{12}) immersed in HCl acid solution containing 11.11 V/V% of extract	29.1348 nm	326.284 nm	1.19735 nm
4. Aluminum coupon (D_7) immersed in HCl acid solution containing 15.89 V/V% of extract	53.5673 pm	0.59384 nm	1.21586 nm
5. Aluminum coupon (D_2) immersed in HCl acid solution containing 20 V/V% of extract	38.5951 pm	0.51183 nm	1.03233 nm
6. Aluminum coupon (D_4) immersed in HCl acid solution containing 23.81 V/V% of extract	21.2896 pm	395.437 pm	957.682 pm

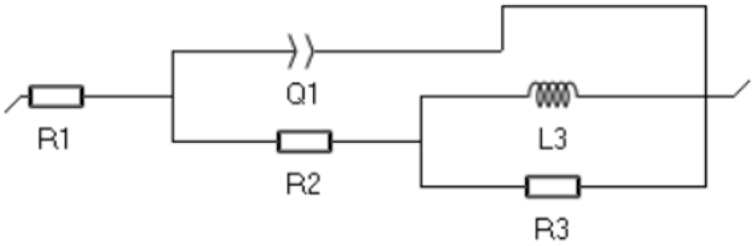

Figure 5: *Equivalent Circuit Model*

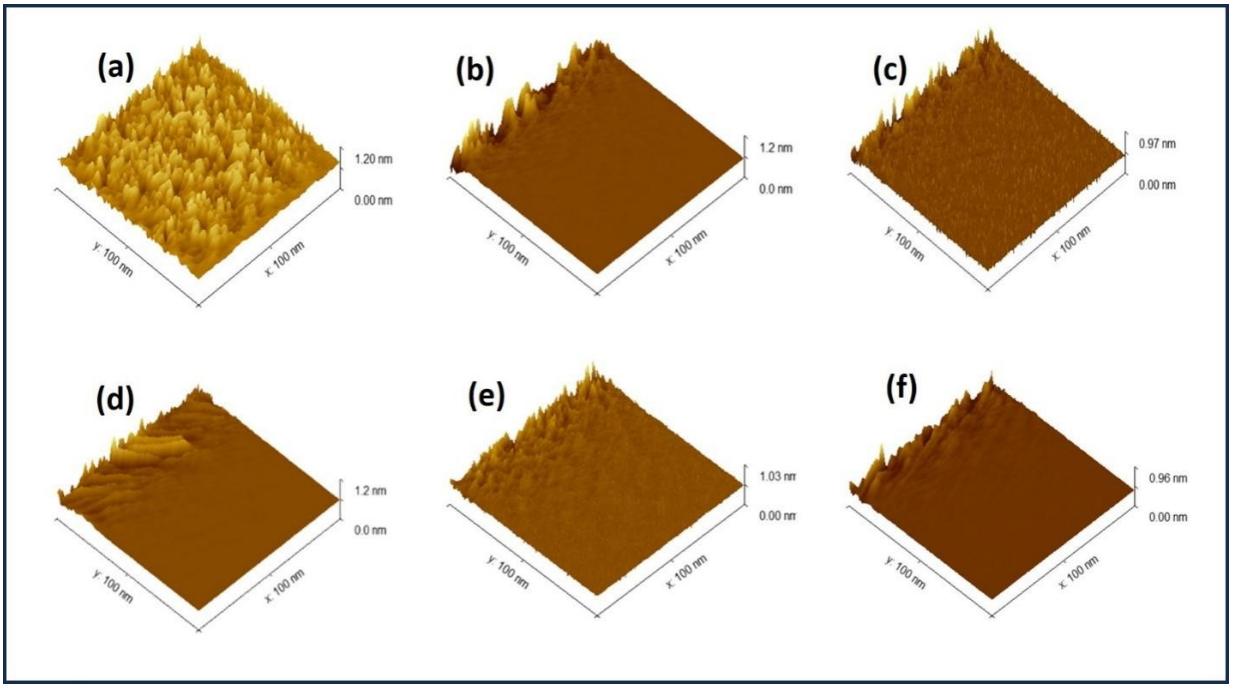

Figure 6: *Image of aluminum coupon after immersion in 0.5 M HCl solution* ***(a)*** *without inhibitor,* ***(b)*** *in the presence of 5.81 V/V% of MPSSE,* ***(c)*** *in the presence of 11.11 V/V% of MPSSE,* ***(d)*** *in the presence of 15.89 V/V% of MPSSE,* ***(e)*** *in the presence of 20 V/V% of MPSSE,* ***(f)*** *in the presence of 23.81 V/V% of MPSSE*

The high and stable impedance at low frequencies suggests a capacitive or resistive nature, where the system can store charge. The significant drop in impedance and steep decline in phase angle in the mid-frequency range indicate the presence of reactive elements (inductive or capacitance) that dominates the response. Inhibition in the Al inhibitor sample is evident through the distinct changes in both the magnitude and phase plots compared to the Al Blank sample. In the magnitude plot, as the frequency increases, the impedance for the Al inhibitor decreases significantly from 1 Hz to 100 Hz, compared to a more gradual decrease for Al Blank from 10 Hz to 1 kHz. From the phase plot, as frequency increases, the phase angle for Al inhibitor decreases more gradually to around 70^{o} from 1 Hz to 100 Hz, whereas for Al Blank, it drops steeply to around -80^{o} from 10 Hz to 1 kHz. At high frequencies, the phase angle for Al inhibitor approaches 0^{o}, indicating more resistive behavior.

Fig. 5, shows that for this system, an appropriate equivalent circuit model would include elements to represent the solution resistance (R_s), charge transfer resistance (R_{ct}), double-layer capacitance (C_{dl}), and an inductance (L) to account for the inductive behavior observed at low frequencies. Overall, the inhibitor increases the charge transfer resistance and introduces more pronounced inductive behavior, suggesting the formation of a protective layer and more complex

electrochemical interactions on the aluminum surface.

3.5. Surface morphology

AFM is an effective instrument for examining surface morphology at the nano-to-micro scale, and it is now a popular option for determining how inhibitors affect the rate at which corrosion occurs at the metal/solution interface [48]. Fig. 6 shows the three-dimensional (3D) AFM morphologies of the aluminum surface immersed in hydrochloric acid solution with varied concentrations of the extract, the aluminum surface immersed in hydrochloric acid (without inhibitor), and the aluminum surface immersed in hydrochloric acid containing varied concentrations of the MPSSE.

The findings from the AFM image analysis comprised the following: the average roughness (average deviation of all point roughness profile from a mean line over the evaluation length) [49] , the maximum height (Sz) values (vertical distance between the highest peak and the lowest valley within the analyzed area of the surface) [50], (and the root-mean-square roughness (Sq) (the average of the measured height deviations taken within the evaluation length and measured from the mean line). These values are compiled in Table 2 for the various aluminum surfaces immersed in different environments.

Significant variations in surface roughness characteristics are shown by the AFM results in Table 2 for the aluminum coupons immersed in HCl solution and different doses of the MPSSE demonstrating the extract's potency as a corrosion inhibitor. The highest values of RMS roughness (183.917 pm), average roughness (0.56355 nm), and maximum height (1.34769 nm) were displayed by the submerged sample in HCl solution without the extract, showing significant corrosion. This is also demonstrated in Fig. 6a. On the other hand, the samples that were immersed in HCl media containing the extract showed lower values of these parameters.

This is observed in Fig. 3b – Fig. 3f, which display flatter, more homogenous and uniform surfaces than that of the surface without the inhibitor. The results further reveal a general improvement in the surface characteristics of the samples immersed in the inhibitor as the concentration of the inhibitor increased. These findings further prove the efficacy of the MPSSE in inhibiting the corrosion of aluminum metal in hydrochloric acid solution.

4. CONCLUSION

This study evaluated the MPSSE as a potential corrosion inhibitor for aluminum. The GC-MS analysis identified several key compounds ranging from long-chain alkanes to fluorinated compounds, which play a crucial role in corrosion inhibition. These compounds form protective layers on metal surfaces, effectively shielding them from corrosion agents. Weight loss measurements demonstrated that the MPSSE significantly reduced corrosion rates, with the highest inhibition efficiency of 90.73% observed at a 20 V/V% concentration on the 12th day of experimentation. This shows the extract's potent ability to minimize weight loss and corrosion rates compared to the control. The Temkin adsorption isotherm indicated strong adherence of the extract to the metal surface. AFM analysis further confirmed that increasing extract concentrations resulted in smoother metal surfaces. EIS analysis indicated a stable protective layer on the metal surface resulting from increased charge transfer resistance and inductive behavior in the presence of the extract. Overall, the *Musa paradisiaca* stem sap extract shows considerable promise as an eco-friendly and effective corrosion inhibitor.

Acknowledgement

The authors are grateful to the Department of Chemical Engineering, Federal University of Technology, and the Africa Center of Excellence in Future Energies and Electrochemical Systems for allowing us the use of their laboratory facilities.

REFERENCES

[1] S.Mridha (2016) Metallic Materials. In Reference Module in Materials Science and Materials Engineering. Elsevier. https://doi.org/10.1016/B978-0-12-803581-8.040972

[2] K.Sathyanarayana, M.Puttegowda, S..Rangappa, S.Siengchin, P.Shivanna, S.Nagaraju, M.Somashekara, P.Girijashankar, Y.Girijappa (2023) 3 – Metallic lightweight materials: Properties and their applications. In S. Rangappa, S.Doddamani, S.Siengchin, M.Doddamani (Eds.), Lightweight and Sustainable Composite Materials (pp. 47–67). Woodhead Publishing. https://doi.org/10.1016/B978-0-323-95189-0.00003-2

[3] E.Fernandes, S.Krishanmurthy (2022) Design and analysis of shell and tube heat exchanger. Int. J. Simul, 13, 15. https://doi.org/10.1051/smdo/2022005.

[4] A.Hamadouche, A.Azzi, S.Abboudi, R.Nebbali (2018) Enhancement of heat exchanger thermal hydraulic performance using aluminum foam. Exp. Therm. Fluid Sci, *92*, 1–12.

https://doi.org/10.1016/j.expthermflusci.2017.10.035

[5] A.Prasad, K.Anand (2020) Design & Analysis of Shell & Tube Type Heat Exchanger. Int. J. Eng. Res. Technol 9(01).

https://doi.org/10.17577/IJERTV9IS010215.

[6] P.andakumar, D.Loganathan, D.Nataraja, P.Manikandan (2023) 6—Shell and tube heat exchangers in the food industry. In S. M. Jafari (Ed.), *Thermal Processing of Food Products by Steam and Hot Water* (pp. 153–179). Woodhead Publishing. https://doi.org/10.1016/B978-0-12-818616-9.00004-3

[7] P.Wildi-Tremblay, L.Gosselin (2007). Minimizing shell-and-tube heat exchanger cost with genetic algorithms and considering maintenance. Int. J. Energy Res, 31(9), 867– 885.

https://doi.org/10.1002/er.1272

[8] S.Bari, S.Hossain (2013). Waste heat recovery from a diesel engine using shell and tube heat exchanger. Appl. Therm. Eng, *61*(2), 355–363. https://doi.org/10.1016/j.applthermaleng.2013.08.020

[9] V.Pandiyarajan, M.Chinna Pandian, E.Malan, R.Velraj, R.Seeniraj (2011) Experimental investigation on heat recovery from diesel engine exhaust using finned shell and tube heat exchanger and thermal storage system. Appl. Energy *88*(1), 77–87.

https://doi.org/10.1016/j.apenergy.2010.07.023

[10] R.Thakar, S.Bhosle, S.Lahane (2018). Design of Heat Exchanger for Waste Heat Recovery from Exhaust Gas of Diesel Engine. *Procedia Manufacturing*, *20*, 372–376.

https://doi.org/10.1016/j.promfg.2018.02.054

[11] B.Kilkovsky, P.Stehlik, Z.Jegla, L.Tovazhnyansky, O.Arsenyeva, P.Kapustenko (2014) Heat exchangers for energy recovery in waste and biomass to energy technologies – I. Energy recovery from flue gas. Appl. Therm. Eng., *64*(1), 213–223.

https://doi.org/10.1016/j.applthermaleng.2013.11.041

[12] R.Shah, B.Thonon, D.Benforado (2000) Opportunities for heat exchanger applications in environmental systems. Appl. Therm. Eng., *20*(7), 631–650.

https://doi.org/10.1016/S1359-4311(99)00045-9

[13] M.Mehdizadeh, F.Pourfayaz, A.Kasaeian, M.Mehrpooya (2017) A practical approach to heat exchanger network design in a complex natural gas refinery. Nat. Gas Sci. Eng., *40*, 141–158. https://doi.org/10.1016/j.jngse.2017.02.001

[14] W.Faes, S.Lecompte, Z.Ahmed, J.Bael, R.Salenbien, K.Verbeken, M.Paepe (2019) Corrosion and corrosion prevention in heat exchangers. Corros. Rev., *37*(2), 131–155.

https://doi.org/10.1515/corrrev-2018-0054.

[15] [M.Ali, A.Ul-Hamid, T.Khan, A.Bake, H.Butt, O.Bamidele, A.Saeed (2021) Corrosion-related failures in heat exchangers. Corros. Rev., *39*(6), 519–546. https://doi.org/10.1515/corrrev-2020-0073

[16] J.Stringer (2004) High temperature corrosion issues in energy-related systems. Mater., *7*, 01–19. https://doi.org/10.1590/S1516-14392004000100002

[17] K.Li, Y.Zeng (2022) Corrosion of heat exchanger materials in co-combustion thermal power plants. Renew. Sust. Energ. Rev, *161*, 112328.

https://doi.org/10.1016/j.rser.2022.112328

[18] J.Kaufman (2019) Corrosion of Aluminum and Aluminum Alloys. In K. Anderson, J. Weritz, & J. G. Kaufman (Eds.), *Properties and Selection of Aluminum Alloys* (pp. 96–129). ASM International. https://doi.org/10.31399/asm.hb.v02b.a0006546.

[19] S.Addepalli, D.Eiroa, S.Lieotrakool, A-L.François, J.Guisset, D.Sanjaime, M.Kazarian, J.Duda, R.Roy, P.Phillips (2015) Degradation Study of Heat Exchangers. *Procedia CIRP*, *38*, 137–142. https://doi.org/10.1016/j.procir.2015.07.057

[20] C.Penot, D.Martelo, S.Paul (2023) Corrosion and Scaling in Geothermal Heat Exchangers. Appl. Sci.*13*(20), Article 20. https://doi.org/10.3390/app132011549.

[21] G.khan, S.Newaz, W..Basirun, H.Ali, F.Faraj, G.Khan (2015) Application of Natural Product Extracts as Green Corrosion Inhibitors for Metals and Alloys in Acid Pickling Processes-A review. Int. J. Electrochem. 10(8), 6120–6134. https://doi.org/10.1016/S1452-3981(23)06707-X

[22] J-W.Lee, W.Hwang (2018) Fabrication of a superhydrophobic surface with fungus-cleaning properties on brazed aluminum for industrial application in heat exchangers. Appl. Surf. Sci, *442*, 461–466. https://doi.org/10.1016/j.apsusc.2018.02.170

[23] R.Naderi, M.Fedel, T.Urios, M.Poelman, M-G.Olivier, F.Deflorian (2013) Optimization of silane sol–gel coatings for the protection of aluminium components of heat exchangers. Surf. Interface Anal, *45*(10), 1457–1466. https://doi.org/10.1002/sia.5249

[24] Y-S.Kim, I-J.Park, J-G.Kim (2019) Simulation Approach for Cathodic Protection Prediction of Aluminum Fin-Tube Heat Exchanger Using Boundary Element Method. *MTL*, *9*(3), Article 3. https://doi.org/10.3390/met9030376

[25] A.Patel (2023) Heat Exchanger Materials and Coatings: Innovations for Improved Heat Transfer and Durability. Int. J. Eng. Res. Appl*s*, *13*, 131–142. https://doi.org/10.9790/9622-1309131142

[26] I.Obot, A.Meroufel, I.Onyeachu, A.Alenazi, A.Sorour (2019) Corrosion inhibitors for acid cleaning of desalination heat exchangers: Progress, challenges and future perspectives. J. Mol. Liq., *296*, 111760. https://doi.org/10.1016/j.molliq.2019.111760

[27] I.Onyeachu, M.Solomon, S.Umoren, I.Obot, A.Sorour (2020) Corrosion inhibition effect of a benzimidazole derivative on heat exchanger tubing materials during acid cleaning of multistage flash desalination plants. *Desalination*, *479*, 114283. https://doi.org/10.1016/j.desal.2019.114283

[28] H.Assad, A.Thakur, A.Bharmal, S.Sharma, R.Ganjoo, S.Kaya (2022) 2 Corrosion inhibitors: Fundamental concepts and selection metrics. In *2 Corrosion inhibitors: Fundamental concepts and selection metrics* (pp. 19–50). De Gruyter. https://doi.org/10.1515/9783110760583-002

[29] S.Abo El-Enin, A.Amin (2020) *Review of Corrosion Inhibitors for Industrial Applications*. *3*, 127–145.

[30] M.Chigondo, F.Chigondo (2016) Recent Natural Corrosion Inhibitors for Mild Steel: An Overview. J. Chem, *2016*, 6208937.

https://doi.org/10.1155/2016/6208937

[31] Z.Shang, J.Zhu (2021) Overview on plant extracts as green corrosion inhibitors in the oil and gas fields. J. Mater. Res. Technol., *15*, 5078–5094. https://doi.org/10.1016/j.jmrt.2021.10.095

[32] R.Haldhar, D.Prasad, I.Bahadur, O.Dagdag, S.Kaya, D.Verma, S.Kim (2021) Investigation of plant waste as a renewable biomass source to develop efficient, economical and eco-friendly corrosion inhibitor. J. Mol. Liq., *335*, 116184.

https://doi.org/10.1016/j.molliq.2021.116184

[33] A.Thakur, H.Assad, S.Kaya, A.Kumar (2022) Chapter17—Plant extracts as environmentally sustainable corrosion inhibitors II. In L. Guo, C. Verma, & D. Zhang (Eds.), *Eco-Friendly Corrosion Inhibitors* (pp. 283–310). Elsevier. https://doi.org/10.1016/B978-0-323-91176-4.00017-9

[34] C.Verma, H.Ebenso, I.Bahadur, M.Quraishi (2018) An overview on plant extracts as environmental sustainable and green corrosion inhibitors for metals and alloys in aggressive corrosive media. J. Mol. Liq., *266*, 577–590. https://doi.org/10.1016/j.molliq.2018.06.110.

[35] C.Verma, E.Ebenso, M.Quraishi (2019) Alkaloids as green and environmental benign corrosion inhibitors: An overview. Int. J. Corros. Scale Inhib., *8*(3), 512–528. https://doi.org/10.17675/2305-6894-2019-8-3-3

[36] M.Shamsuzzaman, K.Kalaiselvi, M.Prabakaran (2021) Evaluation of Antioxidant and Anticorrosive Activities of Ceriops tagal Plant Extract. Appl. Sci., *11*(21), Article 21.

https://doi.org/10.3390/app112110150.

[37] A.Rahim, J.Kassim (2008) Recent Development of Vegetal Tannins in Corrosion Protection of Iron and Steel. Recent Pat. Mater. Sci., *1*(3), 223–231.

[38] Y.Shirmohammadli, D.Efhamisisi, A.Pizzi (2018) Tannins as a sustainable raw material for green chemistry: A review. Ind Crop Prod, *126*, 316–332. https://doi.org/10.1016/j.indcrop.2018.10.034.

[39] A.Pal, R.Sarkar, K.Karmakar, M.Mondal, B.Saha (2022). Surfactant as an anti-corrosive agent: A review. *Tenside Surfactants Detergents*, *59*(5), 363–372. https://doi.org/10.1515/tsd-2022-2434

[40] K.Ajijolakewu, A.Ayoola, T.Agbabiaka, F.Zakariyah, N.Ahmed, O.Oyedele, A.Sani (2021) A review of the ethnomedicinal, antimicrobial, and phytochemical properties of Musa paradisiaca (plantain). Bull. Natl. Res. Cent. *45*(1), 86. https://doi.org/10.1186/s42269-021-00549-3.

[41] B.Oyeyinka, A.Afolayan (2019) Comparative Evaluation of the Nutritive, Mineral, and Antinutritive Composition of Musa sinensis L. (Banana) and Musa paradisiaca L. (Plantain) Fruit Compartments. *Plants*, *8*(12), Article 12. https://doi.org/10.3390/plants8120598.

[42] S.Akinyemi, I.Aiyelaagbe, E.Akyeampong (2010) Plantain (Musa Spp.) Cultivation In Nigeria: A Review of Its Production, Marketing And Research In the Last Two Decades. *Acta Horticulturae*, *879*, 211–218. https://doi.org/10.17660/ActaHortic.2010.879.19.

[43] S.Uzairu, M.Kano (2021) Assessment of phytochemical and mineral composition of unripe and ripe plantain (Musa paradisiaca) peels. Afr. j. food sci., *15*(3), 107–112. https://doi.org/10.5897/AJFS2017.1680/

[44] I.Ekeke, S.Umosah, A.Nkwocha (2021) *Musa Paradisiaca* (Plantain) Stem Sap Extract as a Potential Corrosion Inhibitor on Mild Steel in Acid Medium. Int. J. Innov. Sci. Res. Technol.*, 6 (12), 659 - 664.*

[45] K.Amutha, U.Selvakumari (2016) Wound healing activity of methanolic stem extract of Musa paradisiaca Linn. (Banana) in Wistar albino rats. Int. Wound J., *13*(5), 763. https://doi.org/10.1111/iwj.12371

[46] E.Ituen, O.Akaranta, A.James (2016) Evaluation of performance of corrosion inhibitors using adsorption isotherm models: An overview. Am. Chem. Sci. J. *Doi.10.9734/ACSJ/2016/28976*. https://doi.org/10.9734/ACSJ/2016/28976

[47] S.Mitra, N.Sarkar, A.Barik (2017) Long-chain alkanes and fatty acids from Ludwigia octovalvis weed leaf surface waxes as short-range attractant and ovipositional stimulant to Altica cyanea (Weber) (Coleoptera: Chrysomelidae). B. Entomol. Res. *107*(3), 391–400. https://doi.org/10.1017/S0007485316001012.

[48] P.Dohare, K.Ansari, M.Quraishi, I.Obot (2017) Pyranpyrazole derivatives as novel corrosion inhibitors for mild steel useful for industrial pickling process: Experimental and Quantum Chemical study. In Y.Qiang, S.Zhang , B.Tan, S.Chen (2017) Evaluation of Ginkgo leaf extract as an eco-friendly corrosion inhibitor of X70 steel in HCl solution. Corrs. Sci., 133, 6 – 16. https://doi.org/10.1016/j.corsci.2018.01.008

[49] V.Banu, S.Rajendran, S.Abuthahir (2017). International Journal of Chemical Concepts Corrosion Inhibition by Self-assembling Nano films of Tween 60 on Mild steel surface. International Journal of Chemical Concepts, *03*, 161–173.

[50] J.Smith, S.Breakspear, S.Campbell (2003) AFM in surface finishing: Part II. Surface roughness. Trans. Inst. Met. Finish., *81*, B55–B58. https://doi.org/10.1080/00202967.2003.11871499

IZVOD

MUSA PARADISIACA SAP KAO INHIBITOR KOROZIJE ZA ZAŠTITU ALUMINIJUMA U KISELOJ SREDINI

Ova studija istražuje efikasnost ekstrakta stabljike Musa paradisiaca (MPSSE) kao zelenog inhibitora korozije za aluminijum u hlorovodoničnom okruženju. Gasna hromatografija-masena spektroskopija (GC-MS) identifikovala je jedinjenja u ekstraktu. Potencijal inhibicije korozije je procenjen gravimetrijskom analizom (merenja gubitka težine) i spektroskopijom elektrohemijske impedanse (EIS). Analiza površine je sprovedena korišćenjem mikroskopije atomske sile (AFM) da bi se ispitala morfologija površine aluminijuma pre i posle tretmana. Studije izoterme adsorpcije su sprovedene da bi se razumeo mehanizam interakcije između ekstrakta i površine aluminijuma , koristeći Langmuir , Temkin, Frumkin i Freundlich izoterme. Rezultati pokazuju da ekstrakt pokazuje potencijal inhibicije korozije. GC-MS analiza identifikovala je jedinjenja kao što su dugolančani alkani, estri ftalne kiseline i fluorovana jedinjenja, koja doprinose otpornosti na koroziju formiranjem zaštitnih barijera na metalnim površinama. Gravimetrijska analiza je pokazala da je ekstrakt , posebno pri koncentraciji od 20 V/V%, postigao efikasnost inhibicije do 90,73% tokom 30 dana, značajno smanjujući gubitak težine i stope korozije . Studije adsorpcije su otkrile snažno pridržavanje Temkin Isotherm modela, što sugeriše efikasnu adsorpciju ekstrakta na površini aluminijuma . Mikroskopija atomske sile pokazala je smanjenje hrapavosti površine sa povećanjem koncentracije ekstrakta , potvrđujući zaštitni efekat inhibitora . Spektroskopija elektrohemijske impedanse pokazala je veću otpornost na prenos naelektrisanja i izraženo induktivno ponašanje sa inhibitorom, što ukazuje na formiranje zaštitnog sloja na aluminijumu. Nalazi ističu potencijal MPSSE-a kao ekološki prihvatljive alternative za zaštitu od korozije u industrijskim aplikacijama.

Ključne reči: *inhibitor korozije: gravimetrijska analiza; Musa paradisiaca; elektrohemijska impedansna spektroskopija, ekološki prihvatljiva alternativa.*

Naučni rad
Rad primljen: 13.10.2024.
Rad prihvaćen: 21.11.2024.

Ifeyinwa C. Ekeke https://orcid.org/0000-0002-8165-4449
Chukwuebuka E. Mgbemere https://orcid.org/0009-0004-5165-460X
Charity N. Nwanze https://orcid.org/0000-0002-7585-9050
Chinedu F. Aniukwu https://orcid.org/0009-0008-5376-7148
Chigoziri N. Njoku https://orcid.org/0000-0002-8999-3912